MR Physics for Physicists - NMR Physics: Firming up the Foundations

Douglas C. Noll, Ph.D., Department of Biomedical Engineering, University of Michigan
dnoll@umich.edu, http://www.bme.umich.edu/labs/dnoll/

HIGHLIGHTS

- The Bloch Equations can be rewritten into the rotating frame, making it much easier to visualize the effects of applied rotating magnetic field used for excitation.
- The small tip angle approximation is very useful for understanding slice profile and multidimensional excitation.
- Excitation k-space, similar to k-space for image acquisition, is a concept that can be used to design complicated patterns of excitation.
- There are some nuances and interesting extensions when designing RF pulses for large tip angle (> 90 degrees) excitation.

TALK TITLE: **Bloch Equation in the Rotating Frame, Excitation and Multidimensional Excitation**

TARGET AUDIENCE: Graduate students and recent Ph.D.'s in engineering and natural science and MR physicists with an interest in designing pulse sequences including excitation pulses

OUTCOMES/OBJECTIVES: Students should gain a better understanding of Bloch equations as they relate to excitation and learn general principles and approaches for design of one-dimensional and multidimensional excitation RF pulses.

PURPOSE: The main purpose of the presentation is to provide a better understanding of the behavior of magnetization under applied magnetic fields, such as RF pulses and gradient fields. With the mathematical foundation provided by the Bloch equations, one can approach the problem of how to design one- and multiple dimensional, spatially- and spectrally-selective RF pulses for many applications.

THEORY AND METHODS

The Bloch Equations

The Bloch equations govern the behavior of the net magnetization in the presence of applied magnetic fields. The Bloch equations provide the "classical" description of motion of the magnetization vector and does not easily account for some quantum mechanical behavior seen in, for example, coupled spin systems. While simple concepts such as on-resonant energy absorption can help to explain the excitation of a plane of on-resonance spins in slice selection and more detailed analysis is necessary for describing the slice profile and multidimensional excitation.

We start with the Bloch equations, neglecting relaxation:

$$\frac{d\mathbf{M}}{dt} = \mathbf{M} \times \gamma \mathbf{B}$$

where $\mathbf{M} = [m_x\ m_y\ m_z]$' and $\mathbf{B} = [B_x\ B_y\ B_z]$'. This vector equation, while complicated, merely dictates that the magnetization **M** will precess around any **B** field at frequency $\omega = \gamma B$.

Rotating Frame of Reference

One of the more useful tools in simplifying MRI concepts is the rotating frame of reference. Here we consider that our coordinate system for observation of the magnetization is rotating at a frequency, $\omega_0 = \gamma B_0$. In particular, the coordinate system is rotating about the z-axis in the same direction that **M** rotates about **B**. The z coordinate does not change, but we now must define a new x and y coordinate system. The "laboratory" frame of reference is the usual frame of reference with coordinates (x, y, z). The "rotating" frame of reference has coordinates (x', y', z). If we have magnetization precessing at ω_0, it will appear to be stationary in the rotating frame.

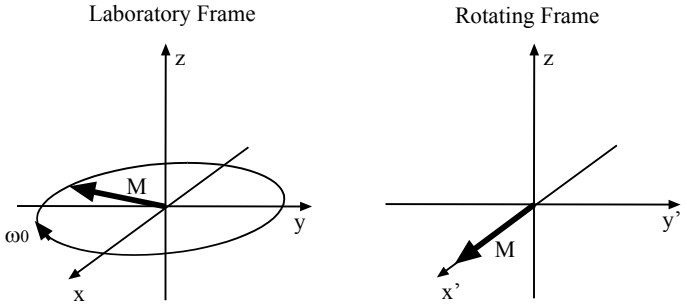

If one has magnetization precessing in the transverse plane, $m_{xy} = m_x + im_y = m_0 \exp(-i\omega_0 t)$, it will appear stationary in the rotating frame: $m_{xy,rot} = m_{x,rot} + im_{y,rot} = m_0$. Conceptually, we can think of this as being similar to riding on a carousel. If we are on the carousel, other objects on the carousel appear stationary, but to someone on the ground, the objects are spinning by at ω_{carousel} (ω_0). The z-component of the magnetization is the same in both frames of reference: $m_{z,rot} = m_z$.

In the rotating frame of references, the magnetization is not precessing. Thus, the apparent or effective **B** in the rotating frame is $\mathbf{B}_{\text{eff}} = 0$. More generally, the rotating frame has an effective z magnetic field that is $\mathbf{B}_0$ less than the applied magnetic field: $B_{z,eff} = B_z - B_0$. Most generally, if we assume that the rotating frame is at ω_{frame}, we can relate the rotating and lab frame magnetization and applied fields are:

$$m_{xy} = m_{xy,rot} \exp(-i\omega_{\text{frame}} t),\ m_{z,rot} = m_z$$
$$B_{xy} = B_{xy,eff} \exp(-i\omega_{\text{frame}} t),\ B_{z,eff} = B_z - \omega_{\text{frame}}/\gamma,$$

along with the Bloch equation in the rotating frame:

$$\frac{d\mathbf{M}_{rot}}{dt} = \mathbf{M}_{rot} \times \gamma \mathbf{B}_{eff}\ .$$

For signal reception, it is interesting to note that the receiver allows you to see magnetization in the rotating frame defined by the frequency of the receive demodulator and thus, we can define the MRI signal equation using $m_{xy,rot}$.

Excitation

Recall, we said that the Bloch equation, which describes the motion of **M** in the presence of a **B** field, dictates that the magnetization will precess around the **B** field at frequency γB. Here, we have two

applied field, B_0 and B_1, and determining the motion of $\mathbf{M}$ in this case can be quite tricky with the Bloch equations. But fortunately, we have a tool to make this analysis easier: the rotating frame.

Let's consider the magnetization starting in its equilibrium position aligned to B_0 (z axis). RF excitation (B_1) that is applied at ω_0 in the lab frame will appear as a stationary $\mathbf{B_{1,eff}}$ is aligned to the *x'* axis in the rotating frame. In the rotating frame, B_0 disappears and one only has to consider B1 and we see that $\mathbf{M_{eff}}$ will precess around *x'* B_1 at frequency $\omega_1 = \gamma B_1$:

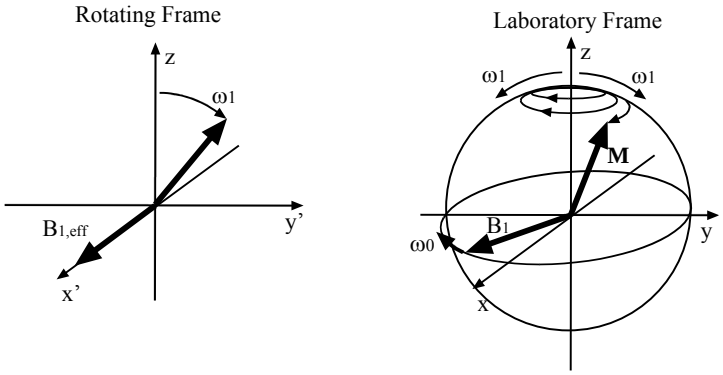

Slice Selective Excitation

The most common excitation pulse used in MRI is the slice selective RF pulse, which is done by applying an frequency selective RF pulse in the presence of a slice selection gradient (commonly z-gradient). Here the resonance frequency varies in the z-direction and the bandpass RF pulse excites only those spins whose resonant frequency lies within the band. We will examine the Bloch equations for this specific case. We will let $B_1(t)$ be a time-varying, real-valued magnetic field rotating at ω_0. For this analysis, we'll let the rotating frame be at $\omega_{frame} = \omega_0$.

$$\mathbf{B_1}(t) = B_1(t)(\cos\omega_0 t\mathbf{i} + \sin\omega_0 t\mathbf{j})$$

$$\mathbf{B}_{1,eff}(t) = B_1(t)\mathbf{i}'$$

where **i**, **j**, and **k** are unit vectors in the x, y, and z directions. A z-gradient is applied, so the component in the z-direction is:

$$\mathbf{B_z}(z) = (B_0 + G_z \cdot z)\mathbf{k}$$

$$\mathbf{B}_{z.,eff}(z) = (G_z \cdot z)\mathbf{k}$$

and the net effective applied field is:

$$\mathbf{B}_{eff} = B_1(t)\mathbf{i}' + (G_z \cdot z)\mathbf{k}$$

The Bloch equation in the rotating frame for this case reduces to the following:

$$\frac{d\mathbf{M_{rot}}}{dt} = \mathbf{M_{rot}} \times \gamma\mathbf{B_{eff}} = \begin{bmatrix} 0 & \gamma G_z z & 0 \\ -\gamma G_z z & 0 & \gamma B_1(t) \\ 0 & -\gamma B_1(t) & 0 \end{bmatrix} \mathbf{M_{rot}}$$

What we would like to know is how the magnetization, $\mathbf{M_{rot}}$, varies as a function of z position following the application of the specified B_1 field. This is, in general, a very difficult equation to solve because it is non-linear.

Small Tip Angle Approximation

One particularly useful approach to the solution to the above Bloch equation is to use the "small tip angle approximation." Here, we assume the B_1 produces a small net rotation angle, say,

$$\int \gamma B_1(t)dt < \frac{\pi}{6} \quad (30°)$$

In this case, we can assume the z component of the magnetization, m_z, is approximately equal to m_0 during the RF pulse. Essentially, we are saying that:

$$\cos\left(\int_0^t \gamma B_1(\tau)d\tau\right) \approx 1$$

Under this assumption ($dm_z/dt = 0$ and $m_z(t) = m_0$), the Bloch equation is then:

$$\frac{d\mathbf{M}_{\mathbf{rot}}}{dt} = \begin{bmatrix} 0 & \gamma G_z z & 0 \\ -\gamma G_z z & 0 & \gamma B_1(t) \\ 0 & \underline{0} & 0 \end{bmatrix} \begin{bmatrix} m_{x,rot} \\ m_{y,rot} \\ \underline{m_0} \end{bmatrix}$$

We now would like to solve for $m_{xy,rot}(z,t) = m_{x,rot}(z,t) + i\, m_{y,rot}(z,t)$. We can then write a differential equation using for the transverse component:

$$\begin{aligned} \frac{dm_{xy,rot}}{dt} &= \frac{dm_{x,rot}}{dt} + i\frac{dm_{y,rot}}{dt} \\ &= \gamma G_z z m_{y,rot} - i\gamma G_z z m_{x,rot} + i\gamma B_1(t)m_0 \\ &= -i\gamma G_z z m_{xy,rot} + i\gamma B_1(t)m_0 \end{aligned}$$

Observe that $i\gamma G_z z$ is a constant with respect to time and thus we have a first order differential equation with a driving function $i\gamma B_1(t)m_0$. For initial condition, $m_{xy,rot}(z,t) = 0$, the solution to this differential equation at the end of the RF pulse (T) can be shown be:

$$m_{xy,rot}(z,T) = im_0 e^{-i\gamma G_z z T}\int_0^T \exp(i\gamma G_z z\xi)\gamma B_1(\xi)d\xi$$

We now make a variable substitution, $s = \xi - T/2$. We can also assume that the RF pulse that is symmetrical (even) around $T/2$ and that it is zero outside of the interval $[0,T]$. The magnetization can now be described as:

$$\begin{aligned} m_{xy,rot}(z,T) &= im_0 e^{-i\gamma G_z z T}\int_{-T/2}^{T/2} \exp(i\gamma G_z z(s+T/2))\gamma B_1(s+T/2)ds \\ &= i\gamma m_0 e^{-i\gamma G_z z T/2}\int_{-T/2}^{T/2} \exp(i\gamma G_z z s)B_1(s+T/2)ds \\ &= i\gamma m_0 e^{-i\gamma G_z z T/2}\int_{-\infty}^{\infty} B_1(s+T/2)\exp\left(i2\pi\left(\frac{\gamma}{2\pi}G_z z\right)s\right)ds \\ &= i\gamma m_0 e^{-i\gamma G_z z T/2} F^{-1}\{B_1(s+T/2)\}\big|_{x=\frac{\gamma}{2\pi}G_z z} \end{aligned}$$

which is the well know Fourier relationship between the RF pulse ($B_1(t)$) and the slice profile. The leading phase term must be compensated for by using a rephaser gradient after the RF pulse.

Multidimensional Excitation and Excitation k-space

We can construct a more general case where the applied gradient fields are along multiple directions and possibly time-varying, $[\mathbf{G}(t)\cdot\mathbf{x}]$, and the applied RF fields can be complex. Here the small tip approximation is:

$$\frac{d\mathbf{M}_{\mathbf{rot}}}{dt} = \gamma \begin{bmatrix} 0 & \mathbf{G}(t)) \cdot \mathbf{x} & -B_{1,y}(t) \\ -\mathbf{G}(t) \cdot \mathbf{x} & 0 & B_{1,x}(t) \\ \underline{0} & \underline{0} & 0 \end{bmatrix} \begin{bmatrix} m_{x,rot} \\ m_{y,rot} \\ \underline{m_0} \end{bmatrix}.$$

Following Pauly [Pauly 1989a], we define $B_1(t) = B_{1,x} + iB_{1,y}$, and the above equation simplifies to:

$$\frac{dm_{xy,rot}}{dt} = -i\gamma[\mathbf{G}(t) \cdot \mathbf{x}]m_{xy,rot} + i\gamma B_1(t)m_0$$

which, for an initial condition with m_0 aligned the B_0, has a solution:

$$m_{xy,rot}(\mathbf{x},T) = i\gamma m_0 \int_0^T B_1(t) \exp\left(-i\gamma\left[\mathbf{x} \cdot \int_t^T \mathbf{G}(s)ds\right]\right)dt \cdot$$

In a manner similar to image k-space, we can define excitation k-space [ref] as:

$$\mathbf{k}(t) = -\gamma \int_t^T \mathbf{G}(s)\mathrm{d}s$$

and then

$$m_{xy,rot}(\mathbf{x},T) = i\gamma m_0 \int_0^T B_1(t) \exp(i[\mathbf{x} \cdot \mathbf{k}(t)])dt \cdot$$

Note that excitation k-space is a time reversed integral of the gradient waveforms, and this forms the pathway upon which the RF energy is deposited in k-space by $B_1(t)$. Note also that since k-space is a time-varying function, there is also in implicit weighting by the inverse of the velocity of through excitation k-space – a slow pathway deposits more B_1 than a fast pathway. Thus, the resultant excitation pattern as two components: 1) a k-space sampling pattern and 2) the excitation weighting defined by the RF waveform ($B_1(t)$) as modified the k-space velocity. More specifically, the sampling term is defined as $S(\mathbf{k}) = \int_0^T {}^3\delta(\mathbf{k}(t) - \mathbf{k})|\dot{\mathbf{k}}(t)|\mathrm{d}t$, where the ${}^3\delta$ is a delta function in 3D that defines the k-space path. The RF weighting term is defined as $W(\mathbf{k}(t)) = B_1(t)/|\gamma\mathbf{G}(t)|$, which is defined only on the k-space pathway. We can then recast the excitation pattern (shown in the previous equation in a time integral) in the k-domain as:

$$m_{xy,rot}(\mathbf{x},T) = i\gamma m_0 \int_{\mathbf{k}} W(\mathbf{k})S(\mathbf{k}) \exp(i[\mathbf{x} \cdot \mathbf{k}])d\mathbf{k} \cdot$$

Thus, for a fully sampled, non-crossing excitation k-trajectory (e.g. an Archimedean spiral) and a desired excitation pattern, $d(\mathbf{x})$, one can define the RF waveform as:

$$B_1(t) = F\{d(\mathbf{x})\}|_{\mathbf{k}=\mathbf{k}(t)} \cdot |\gamma\mathbf{G}(t)|.$$

Below we demonstrate the design of an RF waveform for a spiral excitation k-space trajectory with a Gaussian 2D target profile and the resultant small-tip excitation pattern.

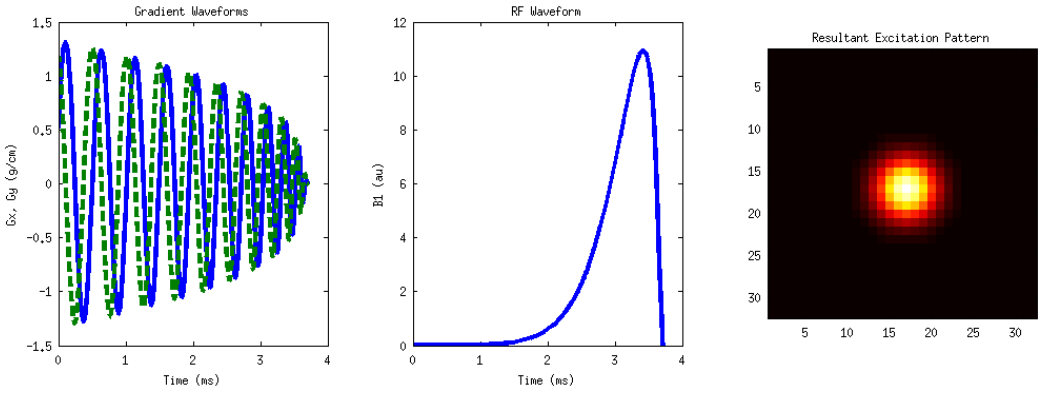

Iterative Methods for Multidimensional RF Pulse Design

The above approach provides an analytical expression for multidimensional RF pulses for a particular k-trajectory and desired pattern, however, this approach has some limitations with respect to the kinds of trajectories that can be easily employed, accounting for magnetic field inhomogeneity, enforcing power constraints, or exploiting spatially limited objects. Here, we describe an iterative pulse design approach developed by Yip et al. [Yip 2005], which is based on a discretization of the above time domain integral:

$$m_{xy,rot}(\mathbf{x},T) \approx i\gamma m_0 \sum_{j=0}^{N-1} B_1(t_j) \exp\left(i\left[\mathbf{x}\cdot\mathbf{k}_j\right]\right)\Delta t$$

which can be rewritten as a simple matrix equation:

$$\mathbf{m} = \mathbf{A}\mathbf{b}$$

where $\mathbf{m}$ is the resultant magnetization, $\mathbf{b}$ is the RF pulse, and $\mathbf{A}$ is a system matrix with elements:

$$a_{ij} = i\gamma m_0 \exp\left(i[\mathbf{x}_i \cdot \mathbf{k}(t_j)]\right)\Delta t$$

where $\mathbf{x}_i$ are voxel locations in the object. Including the magnetic field inhomogeneity $\Delta\omega(\mathbf{x})$ yields:

$$a_{ij} = i\gamma m_0 \exp\left(i[\mathbf{x}_i \cdot \mathbf{k}(t_j)] + i\Delta\omega(\mathbf{x}_i)(t_j - T)\right)\Delta t\,.$$

Using this formalism, we can easily design an RF pulse as a statistical estimation (minimization) problem:

$$\hat{\mathbf{b}} = \underset{\mathbf{b}}{\operatorname{argmin}} \left\{ \|\mathbf{A}\mathbf{b} - \mathbf{d}\|_{\mathbf{W}}^2 + \beta R(\mathbf{b}) \right\}.$$

where $\mathbf{d}$ is the desired spatial excitation pattern and $R(\cdot)$ is a regularization term that can penalize, for example, the sum of the squared RF pulse, which is related to power deposition (SAR). With this form, constraints can be incorporated to limit the peak RF power. The first term in the argument is a W-weighted 2-norm, where the weighting function can be used to ignore voxels with no spins or "don't care" regions. The formalism can handle arbitrary excitation k-trajectories, including variable density and crossing trajectories.

Frequency Spectrum as Another Dimension

We have thus far described multidimensional excitation as 2 or 3 spatial dimensions and that the frequency spectrum is a nuisance term in the form of magnetic field inhomogeneity. However, as described in Meyer et al. [Meyer 1990], one can explicitly consider the spectral frequency dimension as a dimension which we want to control. In the approach, we can define the k-space or Fourier domain equivalent of the spectrum as a simple function of time: $k_\omega = t - T$. The pulse design then proceeds using either direct (with some modification to the k-velocity term) or iterative approaches and the desired pattern ($\mathbf{d}$) is specified in both spatial ($\mathbf{x}$) and frequency (ω) domains. Note that the spectral k-domain (k_ω) is somewhat constrained in that it can only move in the positive direction at a constant velocity and that it can only occupy the negative part of the domain unless spin echo pulses are used. This makes the control of the spectral dimension not quite as robust as the spatial dimension.

Large Tip Angle Extensions

All of the above 1D and multidimensional RF pulse design approaches are based on the small tip angle approximation, but the design of large tip-angle pulses is more complicated. There are many approaches for the design of 1D RF pulses for large tip angles, e.g. for slice selective inversions or spin-echo pulses. One of the more commonly used approaches is the so-call Shinnar-LeRoux algorithm popularized by Pauly et al. [Pauly 1991]. For the design of large-tip angle, multidimensional pulses, Pauly also described an approach that can be used for a series of self-refocused k-trajectories [Pauly 1989b]. A variety of other approaches have been developed to handle the large-tip angle case for multidimensional excitation [Pruessmann 2000, Xu 2007, Xu 2008, Sesompop 2008, Grissom 2008,

Grissom 2009], which include methods for incremental correction to small-tip designs and full non-linear design approaches.

SUMMARY: In the above sections, we described the Bloch equations in the rotating frame and how this simplifies analysis of excitation pulses. We then describe a very powerful approximation – the small tip angle approximation, which allows the use of a Fourier interpretation. Extended to the multiple spatial dimensions, the Fourier interpretation leads to the concept of excitation k-space and to direct and iterative RF pulse design approaches. With this mathematical foundation, one can design one- and multiple dimensional, spatially- and spectrally-selective RF pulses for many applications.

REFERENCES:

Grissom, W. A., Yip, C. Y., Wright, S. M., Fessler, J. A., & Noll, D. C. (2008). Additive angle method for fast large-tip-angle RF pulse design in parallel excitation. *Magnetic Resonance in Medicine*, *59*(4), 779-787.

Grissom, W. A., Xu, D., Kerr, A. B., Fessler, J. A., & Noll, D. C. (2009). Fast large-tip-angle multidimensional and parallel RF pulse design in MRI. *Medical Imaging, IEEE Transactions on*, *28*(10), 1548-1559.

Grissom, W., Yip, C. Y., Zhang, Z., Stenger, V. A., Fessler, J. A., & Noll, D. C. (2006). Spatial domain method for the design of RF pulses in multicoil parallel excitation. *Magnetic resonance in medicine*, *56*(3), 620-629.

Meyer, C. H., Pauly, J. M., Macovskiand, A., & Nishimura, D. G. (1990). Simultaneous spatial and spectral selective excitation. *Magnetic Resonance in Medicine*, *15*(2), 287-304.

Pauly, J., Nishimura, D., & Macovski, A. (1989a). A k-space analysis of small-tip-angle excitation. *Journal of Magnetic Resonance (1969)*, *81*(1), 43-56.

Pauly, J., Nishimura, D., & Macovski, A. (1989b). A linear class of large-tip-angle selective excitation pulses. *Journal of Magnetic Resonance (1969)*, *82*(3), 571-587.

Pauly, J., Le Roux, P., Nishimura, D., & Macovski, A. (1991). Parameter relations for the Shinnar-Le Roux selective excitation pulse design algorithm. *Medical Imaging, IEEE Transactions on*, *10*(1), 53-65.

Pruessmann, K. P., Golay, X., Stuber, M., Scheidegger, M. B., & Boesiger, P. (2000). RF pulse concatenation for spatially selective inversion. *Journal of Magnetic Resonance*, *146*(1), 58-65.

Setsompop, K., Alagappan, V., Zelinski, A. C., Potthast, A., Fontius, U., Hebrank, F., ... & Adalsteinsson, E. (2008). High-flip-angle slice-selective parallel RF transmission with 8 channels at 7T. *Journal of Magnetic Resonance*, *195*(1), 76-84.

Xu, D., King, K. F., Zhu, Y., McKinnon, G. C., & Liang, Z. P. (2007). A noniterative method to design large-tip-angle multidimensional spatially-selective radio frequency pulses for parallel transmission. *Magnetic Resonance in Medicine*, *58*(2), 326-334.

Xu, D., King, K. F., Zhu, Y., McKinnon, G. C., & Liang, Z. P. (2008). Designing multichannel, multidimensional, arbitrary flip angle RF pulses using an optimal control approach. *Magnetic Resonance in Medicine*, *59*(3), 547-560.

Yip, C. Y., Fessler, J. A., & Noll, D. C. (2005). Iterative RF pulse design for multidimensional, small-tip-angle selective excitation. *Magnetic resonance in medicine*, *54*(4), 908-917.